



# Reentrant swelling behavior of thermosensitive *N*-isopropylacrylamide nano-sized gel particles

Sang Chul Jung, Suk Yung Oh, Young Chan Bae\*

Division of Chemical Engineering and Molecular Thermodynamics Lab., Hanyang University, Seoul 133-791, Republic of Korea

## ARTICLE INFO

### Article history:

Received 13 April 2009

Received in revised form

2 May 2009

Accepted 5 May 2009

Available online 18 May 2009

### Keywords:

Modified double lattice model  
Reentrant gel swelling behavior  
*N*-isopropylacrylamide

## ABSTRACT

The closed-loop phase diagram of poly *N*-isopropylacrylamide (PNIPA) in a water–*N,N*-dimethylformamide (DMF) system was measured by thermo-optical analysis (TOA). The reentrant swelling behavior of *N*-isopropylacrylamide (NIPA) nano-sized gel particles in the water–DMF system was measured by using photon correlation spectroscopy (PCS) technique. Theoretically, a modified double lattice model (MDL) can be used to describe the closed-loop phase behavior of linear PNIPA in water–DMF systems. For crosslinked NIPA nano-sized gel particles in a water–DMF system, we combined MDL theory for the mixing contribution and Flory–Erman theory for the elastic contribution. Molecular interaction parameters obtained from the PNIPA solution were used to directly predict the swelling-ratio curves for the NIPA gel. Using our model, the calculated results were in good agreement with the experimental data using only one adjustable parameter.

© 2009 Elsevier Ltd. All rights reserved.

## 1. Introduction

The volume phase transition of hydrogels has recently attracted considerable attention because of its scientific importance and practical applications. Gels undergo a volume phase transition when surrounding conditions such as solvent composition, salt concentration, radiation of UV or visible light, pH, temperature, and type of surfactant are altered [1–12]. These gels have widespread applications in drug delivery systems [13], separation operations in biotechnology, and processing of agricultural products.

In many cases, quick and uniform responses are necessary for successful applications of hydrogels. The rate of response of a given hydrogel is inversely proportional to the square of the size of the gel [14]. Consequently, nano-sized gel particles respond to external stimuli more quickly than bulk gels, and thus are more useful for experiments. Importantly, the swelling behavior of nano-sized gel particles can be measured by photon correlation spectroscopy (PCS). Tanaka et al. [15] reported that nano-sized gel particles exhibit a continuous volume phase transition, while bulk gels have a discontinuous volume phase transition. Further, Yi et al. [16] measured the effect of comonomers with different hydrophobicities on nano-sized polymer gel.

Thermodynamically, crosslinked polymer gels can absorb solvent but are themselves insoluble in the solvent. Thus, the swelling

equilibrium of non-ionic gels is governed by both the free energy of mixing that depends on polymer and solvent interaction with temperature and the elastic forces in the polymer network that counteract swelling. Two types of gels exist, namely, thermoswelling gels and thermoshrinking gels. Thermoswelling type gels follow a UCST phase diagram, collapsing at low temperatures and swelling as the temperature rises. Conversely, thermoshrinking type gels follow a LCST phase diagram and exhibit inverse behavior with respect to thermoswelling type gels. In the past decade, an unusual feature of the re-swelling phenomenon was investigated using acrylamide-derivative copolymer gels created with several different concentrations of dimethyl sulfoxide (Me<sub>2</sub>SO) [9]. Wada et al. [17] reported on the thermosensitive reentrant swelling behaviors of various *N*-(alkoxyalkyl)acrylamide gels and investigated the relationship between the swelling behavior and monomer structures of these gels. Melekaslan and Okay [18] also reported reentrant phase transition of hydrophobically modified hydrogels in aqueous solutions of poly(ethylene glycol)s (PEG) of various molecular weights.

Numerous thermodynamic models for polymer gels require parameters that are either different from those for polymer solutions [19,20] or use too many adjustable parameters [21–23]. Previous work has been done to simultaneously represent the phase behavior of polymer solutions and that of polymer gels using the same parameters [24]. This previous work obtained the interaction energy parameters from LCST type liquid–liquid equilibria (LLE) for a poly *N*-isopropylacrylamide (PNIPA) solution and applied these parameters to the swelling equilibria of *N*-isopropylacrylamide (NIPA) gels. A similar theoretical approach for determining the

\* Corresponding author. Tel.: +82 2 2220 0529; fax: +82 2 2296 0568.

E-mail address: [ycbae@hanyang.ac.kr](mailto:ycbae@hanyang.ac.kr) (Y. Chan Bae).

URL: <http://www.inchem.hanyang.ac.kr/lab/mtl>

relationship between closed-loop type LLE of PNIPA solution and reentrant swelling equilibria of NIPA gels has not yet been reported. In addition, thermodynamic models for thermosensitive reentrant swelling behavior are rare and often have insufficient physical meaning due to the unusual features of such models.

Recently, Oh and Bae [25] extended their modified double lattice (MDL) theory [26] for describing closed miscibility loop phase behavior by employing a new specific interaction term.

In the present study, we measured the closed-loop phase diagram of non-crosslinked PNIPA in a water–DMF system using a TOA apparatus and PCS to analyze the reentrant swelling behavior of crosslinked NIPA nano-sized gel particles. We used the MDL model for describing the phase behavior of the PNIPA solution. To describe the swelling behavior of NIPA gel, we used the MDL theory to describe mixing and the Flory–Erman [27] theory to describe elasticity.

In this study, we describe the swelling behavior of a NIPA gel in a water system using molecular interaction parameters obtained from LCST type LLE data for a PNIPA solution. Secondly, we describe the reentrant swelling behavior of a NIPA gel in a water–DMF system using molecular interaction parameters obtained from closed-loop type LLE data for PNIPA in a water–DMF system. Lastly, we also compare an affine network model with a phantom network model for the given nano-sized gel particles.

## 2. Experimental

### 2.1. Materials

Poly *N*-isopropylacrylamide (PNIPA) samples ( $M_w = 20,000$ – $25,000$ ) and *N,N*-dimethylformamide (DMF) were obtained from Sigma–Aldrich. *N*-isopropylacrylamide (NIPA) obtained by Aldrich was used as the monomer for making NIPA gels. *N,N'*-methylenebisacrylamide (BIS,  $M_w = 154.17$ ) obtained by Aldrich was used as the crosslinker for making NIPA gels. A 1% ammonium persulfate (APS) solution by weight was used as the NIPA gel initiator. Tween20 was used as a non-ionic surfactant to stabilize the nanometer gel particles without affecting the swelling behavior.

### 2.2. Phase diagram sample preparation

Phase diagram samples were prepared in separate test tubes. The composition of each sample was precisely measured gravimetrically. The weight fraction of the polymer ranged from 0.06 to 0.14 for the poly *N*-isopropylacrylamide in the water–DMF system (weight ratio = 1:1). Each solution was stirred for approximately 4 h, after which time the solution was transferred to a pyrex tube (i.d. = 1 mm and o.d. = 3 mm). The test tube was then sealed under dry nitrogen gas using a natural gas/oxygen flame with a sufficiently high temperature such that the pyrex tube could be sealed in less than 2 s. Volatilization and contamination of the sample were avoided using the method described by Bae et al. [28].

### 2.3. Phase diagram measurement by TOA technique

The TOA apparatus consisted of a polarizing microscope (OLYMPUS BX40), a heating-cooling stage, a photodiode (Mettler FP 82), and a microprocessor (Mettler FP 90); a PC was used for data acquisition [28].

The heating and cooling stage were designed for observation of the thermal behavior of a sample under the microscope. Luminosity in the observation field was measured with a photodiode and recorded to a PC. The temperature program for a given operation was entered into the microprocessor. This procedure consisted of a starting temperature, a heating and cooling rate, and an end

**Table 1**  
Experimental cloud-point data for PNIPA in a water–DMF system.

Weight fraction	(°C)	(°C)
0.006	24.2	83
0.015	20.8	99.1
0.025	22.9	99.4
0.052	20.9	100.5
0.074	20.2	102.1
0.095	22.7	90.1
0.13	25.7	90
0.14	26.5	78.4

temperature. The temperature of the system varied from 60 °C to 300 °C, with scan rates as low as 0.1 °C/min for both heating and cooling. Using this method, the photodiode was able to quantitatively measure the intensity of the transmitted light as a function of temperature. Data collected in this manner was used to determine the cloud points of the polymer solutions, and their indexes are shown in Table 1.

### 2.4. Measurement of swelling behavior for nano-sized gel by PCS

We prepared nano-sized NIPA gel beads by precipitation polymerization at 70 °C for 4 h with nitrogen gas blowing. Briefly, distilled deionized water (20 ml) was first introduced to a round bottom flask. We then prepared a monomer solution that was made with the water in the flask, NIPA (0.2 g), and BIS (0.011 g). The hydrodynamic diameters of the nano-sized gel particles were measured by PCS technique [16]. The solution containing gel particles was diluted with distilled deionized water and DMF (weight ratio = 1:1), filtered through a syringe fitted with a 0.45 μm (Whatman) pore size filter to obtain an appropriate concentration for the light-scattering measurement, and finally poured into a glass cell.

Multiple scattering with respect to the concentration of nano-sized gel particles may occur because the detection of any light that has been scattered more than once in a sample can cause distortion of the time dependence of the measured correlation function. For a small particle, the intensity of multiple scattering relative to that of single scattering is proportional to  $\langle C \rangle \alpha^6$ , where  $\langle C \rangle$  is the particle number density and  $\alpha$  is the particle radius. Brown et al. [29] reported that the incidence of multiple scattering is small for  $\langle C \rangle \approx 1.7 \times 10^9 \text{ cm}^{-3}$  and  $\alpha = 500 \text{ \AA}$ . Our value  $\langle C \rangle \alpha^6$  was much smaller than that reported by Brown et al., and thus any distortion from multiple scattering in our experiments was deemed negligible. The temperature of the vat in which the cell was immersed was controlled with a circulation bath ranging from 10 °C to 110 °C with a stability of  $\pm 0.05$  °C. The source of the incident light was an argon-ion laser (Lexel Laser Inc., Model 95-1) operating at 514.5 nm and 100 mW intensity. The scattered light was unpolarized and was detected using a photomultiplier tube (PMT, Brookhaven Instruments Co., Model EMI9863) at a scattering angle of 90°. The signal from the PMT, digitized by an amplifier–discriminator, was fed into a digital 8 bits  $\times$  256 channel (maximum) correlator (Brookhaven Instruments Co., Model BI9000AT), which accumulated the time correlation function of the intensity of the scattered light. The time correlation function was calculated and analyzed using the CONTIN method [30,31].

## 3. Model development

### 3.1. Liquid–liquid equilibria for non-crosslinked PNIPA in solvent system

The framework of the lattice model starts with a simple cubic lattice (coordination number  $z = 6$ ) containing  $N_r$  sites. The systems

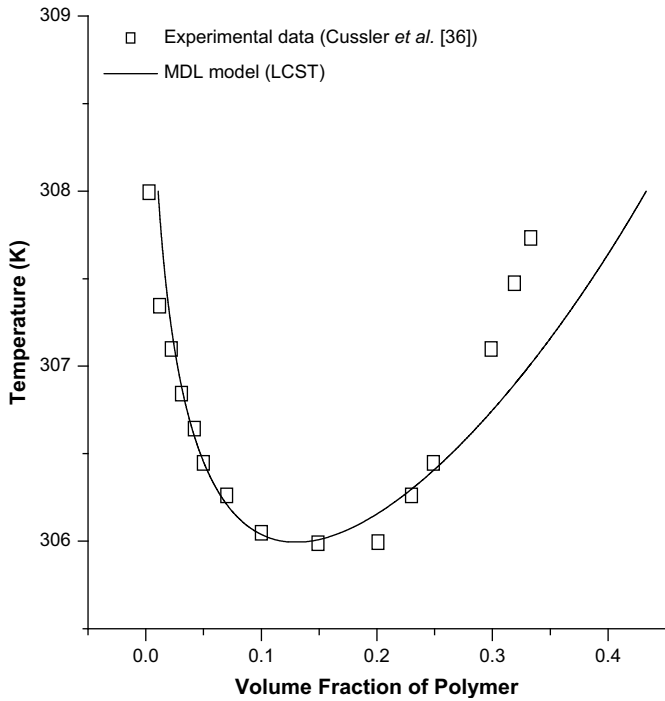


**Fig. 1.** LCST type coexistence curve for PNIPA in a pure water system. The squares represent experimental data from Cussler et al. [36]. The solid line was calculated using the MDL model.

that interact strongly must be correctly oriented in relation to each other, *i.e.*, a specific interaction. Ordinary polymer solutions are described by the primary lattice, while a secondary lattice is introduced as a perturbation to account for oriented interactions.

Oh and Bae [26] defined a new Helmholtz energy of mixing in the form of the Flory–Huggins theory. The expression is given by

$$\frac{\Delta A}{N_r k T} = \left(\frac{\phi_1}{r_1}\right) \ln \phi_1 + \left(\frac{\phi_2}{r_2}\right) \ln \phi_2 + \chi_{OB} \phi_1 \phi_2 \quad (1)$$

where  $N_r$  is the total number of lattice sites (coordination number  $z=6$ ),  $k$  is the Boltzmann constant,  $r_i$  is the number of segments, and  $\phi_i$  is the volume fraction of component  $i$ . The subscripts 1 and 2 refer to the solvent and polymer, respectively. The new interaction parameter  $\chi_{OB}$  is defined by

$$\chi_{OB} = C_\beta \left(\frac{1}{r_2} - \frac{1}{r_1}\right)^2 + \left(2 + \frac{1}{r_2}\right) \tilde{\varepsilon} - \left(\frac{1}{r_2} - \frac{1}{r_1} + C_\gamma \tilde{\varepsilon}\right) \times \tilde{\varepsilon} \phi_2 + C_\gamma \tilde{\varepsilon}^2 \phi_2^2 \quad (2)$$

where  $C_\beta$  and  $C_\gamma$  are universal constants. These constants are determined by the Monte-Carlo simulation data collected by Madden et al. [32]. The best-fit values of  $C_\beta$  and  $C_\gamma$  were 0.1415 and 1.7986, respectively. The term  $\tilde{\varepsilon}$  is a reduced interaction energy parameter given by

$$\tilde{\varepsilon} = \frac{\varepsilon}{kT} = \frac{\varepsilon_{11} + \varepsilon_{22} - 2\varepsilon_{12}}{kT} \quad (3)$$

**Table 2**  
Model parameters for PNIPA in a water system.

System	LLE type	$r_2$	$\varepsilon/k$ (K)	$\delta\varepsilon/k$ (K)
PNIPA in water	LCST	56.0522	1690.05	−1628.58

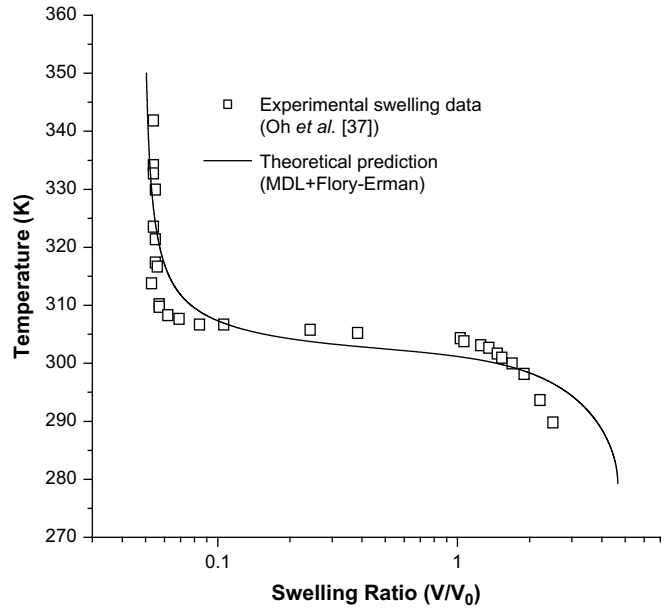


**Fig. 2.** Swelling behavior of a NIPA gel in a pure water system. The squares represent experimental data from Oh et al. [37]. The solid line was calculated using the MDL mixing model combined with the Flory–Erman elastic model.

where  $\varepsilon_{11}$ ,  $\varepsilon_{22}$  and  $\varepsilon_{12}$  are the corresponding nearest neighbor segment–segment interactions.

To improve the mathematical approximation defect and to reduce the number of parameters, a new Helmholtz energy of mixing for the secondary lattice is defined in the fractional form. This expression is given by

$$\frac{\Delta A_{sec,ij}}{N_{ij,kT}} = \frac{2}{z} \left[ \eta \ln \eta + (1-\eta) \ln(1-\eta) + \frac{z C_\alpha \delta \tilde{\varepsilon}_{ij} (1-\eta) \eta}{1 + C_\alpha \delta \tilde{\varepsilon}_{ij} (1-\eta) \eta} \right] \quad (4)$$

where  $\Delta A_{sec,ij}$  is the Helmholtz energy of mixing of the secondary lattice for an  $i-j$  segment–segment pair,  $N_{ij}$  is the number of  $i-j$

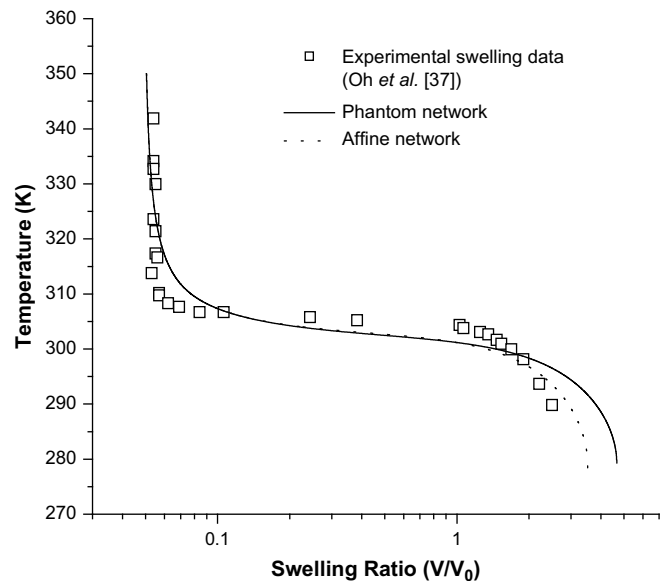


**Fig. 3.** Swelling curve calculated from the corrected MDL model, phantom network model ( $P=1$ ) and affine network model ( $P=10^4$ ).

pairs,  $\delta\tilde{\epsilon}(\delta\epsilon/kT)$  is the reduced energy parameter contributed by the oriented interactions, and  $\eta$  is the surface fraction permitting oriented interactions. For simplicity, we arbitrarily set  $\eta$  to 0.3 as suggested by Hu et al. [33]. The term  $C_\alpha$  is a universal constant that is determined by Gibbs-ensemble Monte-Carlo simulation data of the Ising lattice collected by Panagiotopolus et al. [34]. The best-fit value of  $C_\alpha$  was 0.4881. We used this model to deal with the specific interaction when describing LCST curves.

For aqueous polymer solutions with a closed miscibility loop, strong specific interactions increase with increasing temperatures. Therefore,  $\delta\epsilon$  is separated into two parts to account for the temperature dependence. According to our previous work [26], we replaced  $\delta\epsilon$  with  $\delta\epsilon^H - \delta\epsilon^S T$  in Eq. (4), where  $\delta\epsilon^H$  and  $\delta\epsilon^S$  are enthalpic and entropic energy contributions for the oriented interactions, respectively. Two parameters represent the enthalpic disadvantage,  $\delta\epsilon^H$ , and the entropic advantage,  $\delta\epsilon^S$  for  $\delta\epsilon$  when system temperature increases. We used this model for describing closed-loop type LLE curves.

The secondary lattice contribution is a perturbation to the primary lattice. To incorporate a secondary lattice, we replaced  $\epsilon_{ij}$  with  $\epsilon_{ij} - \Delta A_{sec,ij}/N_{ij}$  in Eq. (3). If oriented interaction occurred in the  $i-j$  segment–segment pairs, we replaced  $\tilde{\epsilon}$  with  $(\epsilon/kT) + 2(\Delta A_{sec,ij}/N_{ij}kT)$  in Eq. (3). If oriented interaction occurred in the  $i-j$  segment–

segment pairs, we replaced  $\tilde{\epsilon}$  with  $(\epsilon/kT) - \Delta A_{sec,ii}/N_{ii}kT$ . In this study, we assumed the oriented interaction occurred only in the  $i-j$  segment–segment pairs.

To calculate the binary coexistence curve, the chemical potential of components 1 and 2 are needed. These chemical potentials are given by

$$\frac{\Delta\mu_1}{kT} = \left[ \frac{\partial(\Delta A/N_r kT)}{\partial N_1} \right]_{T,V,N_2} \quad (5)$$

$$\frac{\Delta\mu_2}{kT} = \left[ \frac{\partial(\Delta A/N_r kT)}{\partial N_2} \right]_{T,V,N_1} \quad (6)$$

A coexistence curve can be determined from the following conditions:

$$\Delta\mu'_1 = \Delta\mu''_1 \quad (7)$$

$$\Delta\mu'_2 = \Delta\mu''_2 \quad (8)$$

where  $\Delta\mu_i$  is the change in chemical potential upon isothermally transferring component  $i$  from the pure state to the mixture.

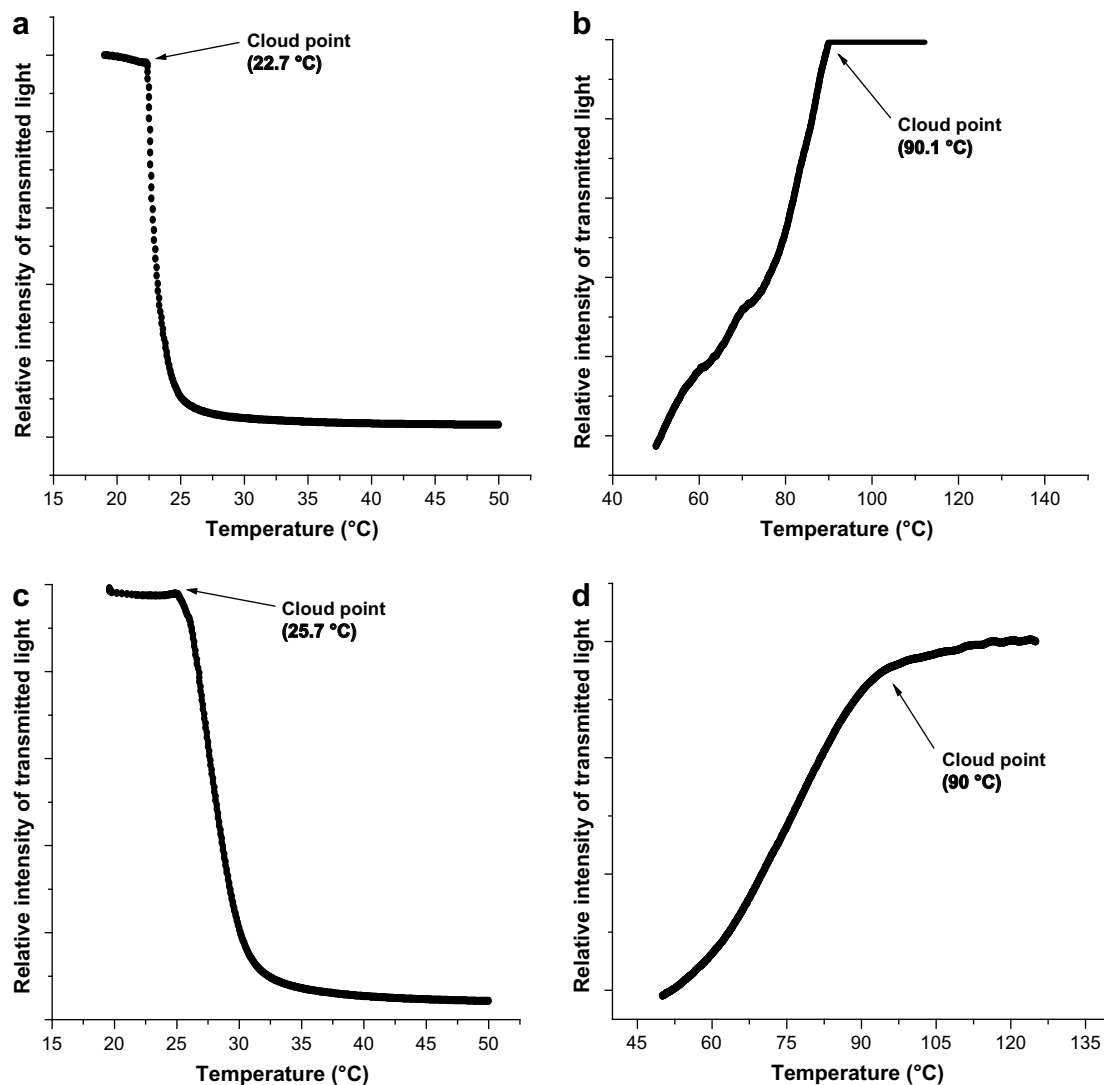


**Fig. 4.** (a) and (b) Cloud-point determination by TOA for PNIPA in a water–DMF system (weight fraction 0.095). (c) and (d) Cloud-point determination by TOA for PNIPA in a water–DMF system (weight fraction 0.13).

Superscripts ' and '' denote two phases at equilibrium. For phase equilibrium calculations, we required the experimental coordinates of the critical point. This critical condition is given by

$$\frac{\partial(\Delta\mu_1/kT)}{\partial\phi_2} = \frac{\partial^2(\Delta\mu_1/kT)}{\partial\phi_2^2} = 0 \quad (9)$$

### 3.2. Swelling behavior for crosslinked NIPA gels

According to Flory [35], the chemical potential of a solvent in a gel phase coexisting with pure solvent is given by

$$\mu_1 - \mu_1^0 = \Delta\mu_1 = \Delta\mu_{1,\text{mix}} + \Delta\mu_{1,\text{ela}} \quad (10)$$

where  $\Delta\mu_{1,\text{mix}}$  and  $\Delta\mu_{1,\text{ela}}$  represent mixing and elastic contributions, respectively.

The mixing contribution  $\Delta\mu_{1,\text{mix}}$  is basically similar to those described above for systems containing non-crosslinked polymer (Eq. (5)). In a system containing a crosslinked polymer network, the  $1/r_2$  term is negligible because  $r_2$ , the segment number of polymer molecules, is considered infinite. Therefore, the chemical potential for a gel system can be simplified as follows:

$$\frac{\Delta\mu_{1,\text{mix}}}{kT} = \ln(1 - \phi_g) + \phi_g + r_1 \left[ \left( C_\beta + \tilde{\epsilon} + C_\gamma \tilde{\epsilon}^2 \right) \phi_g^2 + 2(1 - 2C_\gamma \tilde{\epsilon}) \tilde{\epsilon} \phi_g + 3C_\gamma \tilde{\epsilon}^2 \phi_g^2 \right] \phi_g^2 \quad (11)$$

where  $\phi_g$  is the volume fraction of the gel in the gel phase.

An expression given by Flory and Erman [27] was used to obtain the contribution of elastic forces to the chemical potential. For a perfect tetrafunctional network, the chemical potential for an elastic contribution is given as

$$\frac{\Delta\mu_{1,\text{ela}}}{kT} = \left( \frac{\phi_g^0}{2\chi_c} \right) \lambda^{-1} [1 + K(\lambda)] \quad (12)$$

where

$$K(\lambda) = B \left[ \dot{B}(1+B)^{-1} + (\lambda/\kappa)^2 (B + \lambda^2 \dot{B}) (1 + \lambda^2 B/\kappa)^{-1} \right] \quad (13)$$

and

$$\dot{B} = \partial B / \partial \lambda^2 = B \left[ (\lambda^2 - 1)^{-1} - 2(\lambda^2 + \kappa)^{-1} \right] \quad (14)$$

and  $\lambda$  is the linear swelling ratio

$$\lambda = \left( \frac{V}{V_0} \right)^{1/3} = \left( \frac{\phi_g^0}{\phi_g} \right)^{1/3} \quad (15)$$

where  $V$  and  $V_0$  are the volume of the gel network and the volume in the reference state, respectively.  $\phi_g$  and  $\phi_g^0$  are the corresponding volume fractions of the gel. The network parameter  $\kappa$  relates to  $\chi_c$  and  $\phi_g^0$  as follows:

$$\kappa = \frac{1}{4} P \phi_g^0 \chi_c^{1/2} \quad (16)$$

where the parameter  $\kappa$  represents the constraints on fluctuations of junctions due to the surrounding chains in which they are embedded. If fluctuations due to their embedment in the surrounding randomly configured chains could be suppressed, then  $\kappa = 0$  and the real network approaches a "phantom network" which is the limit of a high degree of swelling. If fluctuations can be suppressed totally by the constraints, then  $\kappa \rightarrow \infty$  and the network is called an "affine network". The dimensionless parameter  $P$  depends

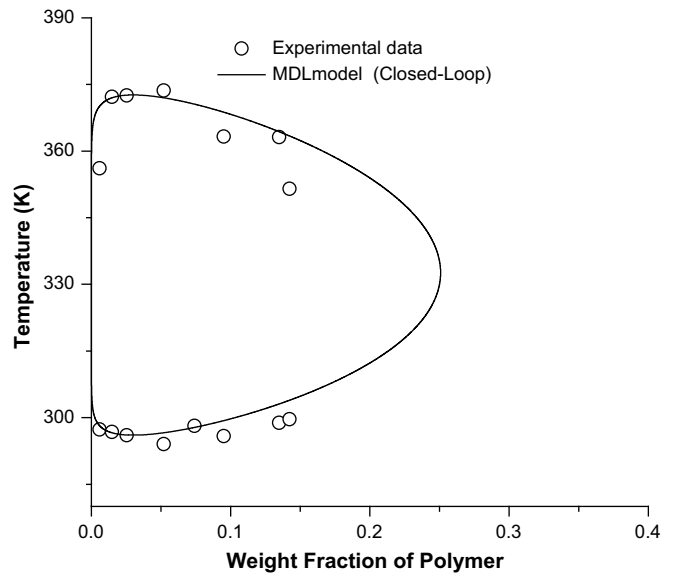


Fig. 5. Closed-loop type coexistence curve for PNIPA in a binary solvent (water-DMF) system. Circles represent experimental data. The solid line was calculated using the MDL model.

on characteristics of the generic type of polymer and the molar volume of the solvent. Here, we assume that the phantom network model is  $P = 1$  and an affine network model is  $P = 10^4$ . The term  $\chi_c$  is the average chain length between crosslinking points. Substituting Eqs. (11) and (12) into Eq. (10), the reduced chemical potential of a solvent in gels can be expressed by

$$\frac{\Delta\mu_1}{kT} = \left( \frac{\phi_g^0}{2\chi_c} \right) \lambda^{-1} [1 + K(\lambda)] + \ln(1 - \phi_g) + \phi_g + r_1 \left[ \left( C_\beta + \tilde{\epsilon} + C_\gamma \tilde{\epsilon}^2 \right) \phi_g^2 + 2(1 - 2C_\gamma \tilde{\epsilon}) \tilde{\epsilon} \phi_g + 3C_\gamma \tilde{\epsilon}^2 \phi_g^2 \right] \phi_g^2 \quad (17)$$

The equilibrium condition for a gel in a solvent system is given by

$$\frac{\Delta\mu_1}{kT} = 0 \quad (18)$$

## 4. Results and discussion

Fig. 1 shows the coexistence curve for PNIPA in a water system [36]; this system exhibits LCST behavior. For this case, we introduced the secondary lattice to account for the specific interaction, and an MDL model was used to calculate the solid line. The calculated curve agreed well with the experimental data, although there was a slight deviation in the polymer rich phase region. The adjustable model parameters are listed in Table 2. Two interaction energy parameters ( $\epsilon/k$ ,  $\delta\epsilon/k$ ) obtained from the linear PNIPA in water system were used directly for the prediction of swelling equilibria for the crosslinked NIPA gel in a water system.

Fig. 2 shows experimental swelling data of nano-sized NIPA gel particles in a pure water system [37] and the theoretical curve calculated from Eqs. (17) and (18). The nano-sized gel particles in this

Table 3  
Model parameters for PNIPA in a water-DMF system.

System	LLE type	$r_2$	$\epsilon/k$ (K)	$\delta\epsilon^H/k$ (K)	$\delta\epsilon^S/k$ (K)
PNIPA in water-DMF	Closed-loop	1257.53	-601.305	10,513.2	15.2426

system were prepared in the presence of solvent and the polymer–solvent interaction was inherently present in the formation of the gel, which led to a perturbed state.  $V_0$  depends on temperature because NIPA gels are thermosensitive, which led to a limitation in determining the reference state. Khokhlov [38] reported that  $V_0$  in the presence of solvent is close to that of the so-called  $\theta$ -temperature. In this work, the state at  $\theta$ -temperature ( $\sim 30.6^\circ\text{C}$ ) [39] for PNIPA in the water system was chosen as a reference state. Alternatively, in cases where the reference state is difficult to determine,  $\phi_g^0$  can be estimated from the experimental asymptotic value of  $V/V_0$  at high temperatures [9], such that  $\phi_g^0 = 0.048$ . The term  $\chi_c$  is estimated from  $C\%$  as follows

$$\chi_c \approx \left( \frac{1}{2\phi_j} \right) \left( \frac{v_m}{v_1} \right) \quad (19)$$

where  $\phi_j$  is the mole fraction of the crosslinker unit to the total monomer unit in the gel network ( $\phi_j \approx C\%/100$ ) and  $v_m$  and  $v_1$  are the molar volumes of monomers and solvent, respectively. In this system, the calculated value of  $\chi_c$  was 256. As mentioned previously, two interaction energy parameters were obtained from correlating LLE for PNIPA in the water system. Thus, the calculated curve shown in Fig. 2 has no fitting adjustable parameter: this curve is a prediction based on the known gel experiment conditions and on the energy parameters obtained from independent experiment. The calculated curve agreed fairly well with the experimental data without adjustable parameters. Fig. 3 shows a comparison of the phantom network model and the affine network model with the swelling data.

Fig. 4(a) and (c) show a typical result for cloud-point determination of a NIPA in a water–DMF system by heating a sample of

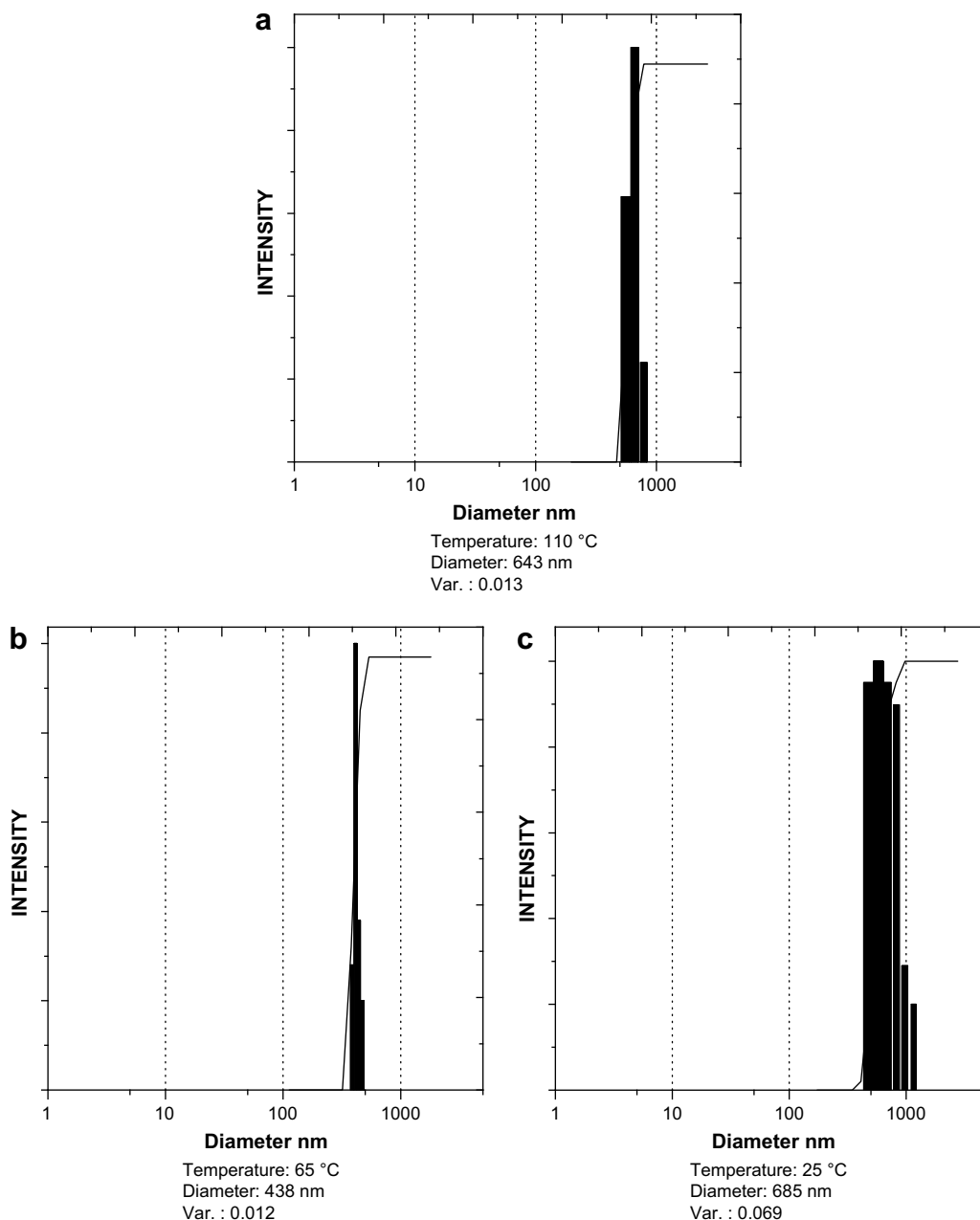
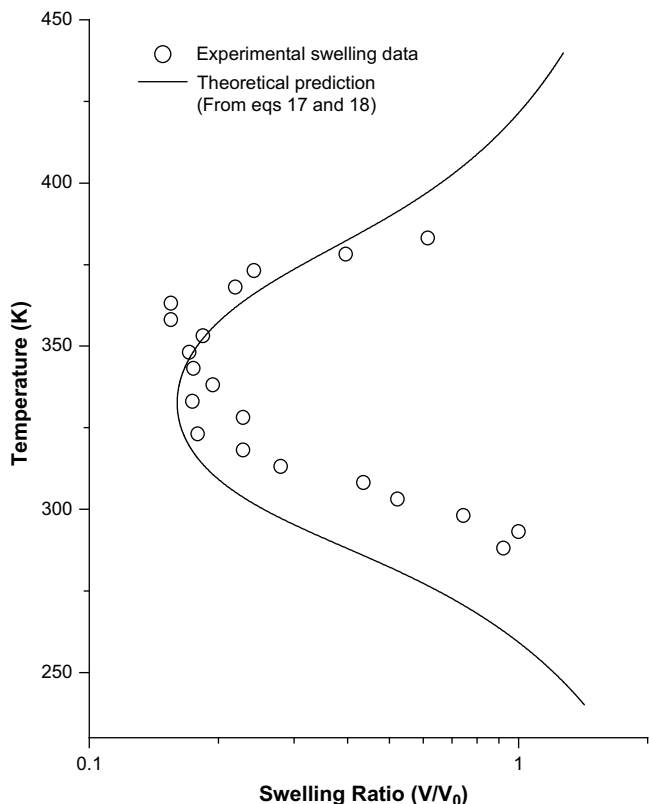


Fig. 6. Particle size distribution with respect to increasing temperature.



**Fig. 7.** Swelling behavior of NIPA gels in a binary solvent (water–DMF) system. Circles represent experimental data. The solid line was calculated using an MDL mixing model combined with the Flory–Erman elastic model.

known polymer weight fraction. The remaining parts of the figure were measured by sample cooling.

Fig. 5 shows a coexistence curve for PNIPA in a water–DMF system which exhibited closed-loop behavior. To apply our binary lattice model to this ternary case, DMF and water were considered to be pseudo pure solvents. Because the ratio of DMF and water was constant and the system composition varied between only polymer (or gel) and pseudo pure solvent, this assumption was thought to be reasonably applicable to our experimental data. In this system, we used corrected secondary lattice terms to account for highly specific interactions. The solid line was calculated by the MDL model. The calculated curve was in good agreement with experimental data, although there was a slight discrepancy between the calculated results and experimental data obtained for the high polymer concentration range. Adjustable model parameters are listed in Table 3. Three interaction energy parameters ( $\varepsilon/k$ ,  $\delta\varepsilon^H/k$ ,

**Table 4**  
Nano-sized gel particle diameters at various temperatures.

Temperature (°C)	Diameter (nm)	Temperature (°C)	Diameter (nm)
15	736	65	438
20	756	70	423
25	685	75	420
30	609	80	430
35	573	85	406
40	494	90	406
45	462	95	456
50	426	100	471
55	462	105	555
60	422	110	643

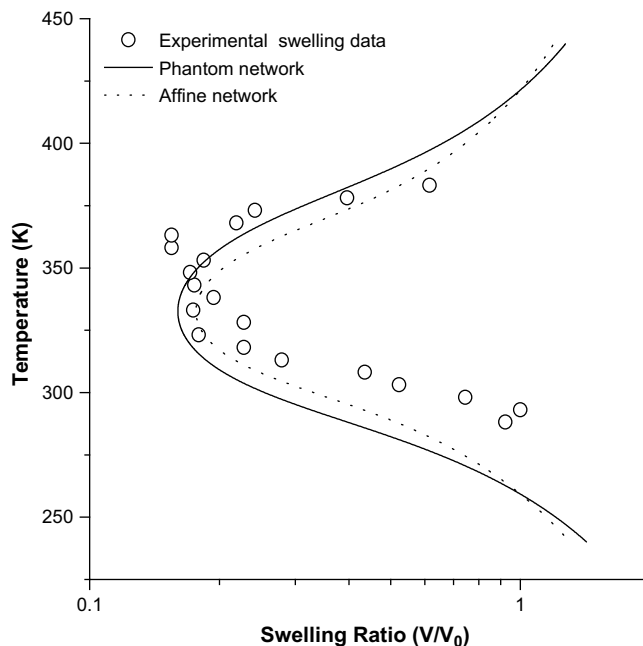


**Fig. 8.** Swelling curve calculated from the corrected MDL model, phantom network model ( $P=1$ ), and affine network model ( $P=10^4$ ).

$\delta\varepsilon^S/k$ ) obtained from the linear PNIPA in the water–DMF system were used directly for the prediction of swelling equilibria for the crosslinked NIPA gels in the water–DMF system.

The results of the PCS measurement of gel particles are shown in Fig. 6. Fig. 7 and Table 4 shows the experimental swelling data of nano-sized NIPA gel particles in the binary solvent (water–DMF) system and the theoretical curve calculated from Eqs. (17) and (18). In this system, the  $\theta$ -temperature and the critical temperature were similar because the critical polymer volume fraction was nearly zero. Therefore, the  $\theta$ -temperature was arbitrarily set to 20 °C, which was slightly lower than the lower critical solution temperature. Likewise, the state at 20 °C was chosen as a reference state. The average hydrodynamic diameters  $D_g^0$  of equilibrium gels at various temperatures were measured by PCS. The volume ratio of nano-sized gel particles was calculated from swelling data as follows

$$\phi_g/\phi_g^0 = V/V^0$$

$$V/V^0 = \left(D/D_g^0\right)^3 \quad (20)$$

where the term  $D_g^0$  represents the reference condition and  $V$  and  $V^0$  are the equilibrium gel volume at the state of interest and the reference state, respectively. The term  $\phi_g^0$  could not be estimated from the experimental asymptotic value of the swelling ratio because the system exhibited re-swelling behavior in the high temperature region. Thus, for this study, we set  $\phi_g^0$  as an adjustable model parameter for fitting swelling data and obtained an acceptable value of 0.04. This value was considered reasonable because the nano-sized gel particles were in a collapsed phase at the reaction temperature. The term  $\chi_c$  was obtained from Eq. (19) and its value was 78.2. As mentioned above, three interaction energy parameters were obtained from correlating LLE for PNIPA in the water–DMF system. Thus, the calculated curve shown in Fig. 7 had only one adjustable parameter ( $\phi_g^0$ ). The calculated curve agreed fairly

well with the experimental data, although it deviated slightly at the highly swollen phase. This deviation may have resulted from the usual assumption that the gel network contained a single type of interaction polymer segment, which as a result disregards the existence of the crosslinker in the gel. Fig. 8 shows the comparison of the phantom network model, the affine network model, and the reentrant swelling data.

## 5. Conclusions

We used a TOA apparatus to measure cloud-point curves for polymer solutions and PCS to measure nano-sized gel particles. The results obtained using the TOA apparatus provided a closed-loop phase diagram for the polymer solution of PNIPA. An MDL model was used to calculate the interaction energy parameter from the closed-loop type LLE for the PNIPA in a water–DMF system. For crosslinked NIPA nano-sized gel particles, we combined MDL theory for the mixing contribution with Flory and Erman theory for elasticity. The independently obtained energy parameters from the MDL model were used directly to predict swelling equilibria for the NIPA gel in a water–DMF system and were in very good agreement with reentrant type experimental swelling data with only one reasonable fitting parameter. In addition, the comparison of the phantom network model and affine network model with the swelling data showed that an affine network model was more appropriate than that of the phantom network model for explaining swelling data.

## Acknowledgments

This work was supported by the Seoul R&BD Program (CR070027).

## References

- [1] Tanaka T. *Phys Rev Lett* 1978;40:820.
- [2] Tanaka T. *Phys Rev Lett* 1978;45:1636.
- [3] Hirowaka Y, Tanaka T. *J Chem Phys* 1984;81:6379.
- [4] Ohmine I, Tanaka T. *J Chem Phys* 1982;77:5752.
- [5] Mamada A, Tanaka T, Kungwachakun D, Irie M. *Macromolecules* 1990;23:1517.
- [6] Suzuki A, Tanaka T. *Macromolecules* 1990;346:345.
- [7] Kokufuta E, Nakaizumi S. *Macromolecules* 1995;28:1704.
- [8] Kokufuta E, Zhang YQ, Tanaka T, Mamada A. *Macromolecules* 1993;26:1053.
- [9] Katayama S, Hirokawa Y, Tanaka T. *Macromolecules* 1984;17:2641.
- [10] Lynch I, Sjöström J, Piculell L. *J Phys Chem B* 2005;109:4252.
- [11] Akala EO, Kopecková P, Kopeček J. *Biomaterials* 1998;19:1037.
- [12] Molina MJ, Gómez-Atón MR, Piérola IF. *J Phys Chem B* 2007;111:12066.
- [13] Brøndsted H, Kopeček J. *Biomaterials* 1991;12:584.
- [14] Tanaka T, Fillore J. *Chem Phys* 1979;70:1214.
- [15] Hirose Y, Amiya T, Hirokawa Y, Tanaka T. *Macromolecules* 1987;20:1342.
- [16] Yi YD, Oh KS, Bae YC. *Polymer* 1997;38:3471.
- [17] Wada N, Yagi Y, Inomata H, Saito S. *Macromolecules* 1992;25:7220.
- [18] Melekaslan D, Okay O. *Macromol Chem Phys* 2001;202:304.
- [19] Hirotsu S, Hirokawa Y, Tanaka T. *J Chem Phys* 1987;87:1392.
- [20] Inomata H, Nagahama K, Saito S. *Macromolecules* 1994;27:6459.
- [21] Prange MH, Hooper HH, Prausnitz JM. *AIChE J* 1989;35:803.
- [22] Oh KS, Bae YC. *J Appl Polym Sci* 1998;69:109.
- [23] Huang Y, Jin X, Liu H, Hu Y. *Fluid Phase Equil* 2008;263:96.
- [24] Hino T, Prausnitz JM. *Polymer* 1998;39:3279.
- [25] Oh SY, Bae YC. *Polymer* 2008;49:4469.
- [26] Oh JS, Bae YC. *Polymer* 1998;39:1149.
- [27] Erman B, Flory PJ. *Macromolecules* 1986;19:2342.
- [28] Bae YC, Lambert SM, Soane DS, Prausnitz JM. *Macromolecules* 1991;24:4403.
- [29] Brown JC, Pusey PN, Ottewill RH. *J Phys A Math Gen* 1975;8:664.
- [30] Chu B. *Laser light scattering*. 2nd ed. NY: Academic Press; 1991.
- [31] Schmitz KS. *An introduction to dynamic light scattering by macromolecules*. NY: Academic Press; 1990.
- [32] Madden WG, Pesci A, Freed KF. *Macromolecules* 1990;23:1181.
- [33] Hu Y, Lambert SM, Soane DS, Prausnitz JM. *Macromolecules* 1991;24:4356.
- [34] Panagiotopoulos AZ, Quirke N, Stapleton M, Tildesley DJ. *Mol Phys* 1998;63:527.
- [35] Flory PJ. *Principles of polymer chemistry*. Ithaca NY: Cornell University Press; 1953.
- [36] Marchetti M, Prager S, Cussler EL. *Macromolecules* 1990;23:3445.
- [37] Oh KS, Oh JS, Choi HS, Bae YC. *Macromolecules* 1998;31:7328.
- [38] Khokhlov AR. *Polymer* 1980;21:376.
- [39] Wu C, Zhou S. *Macromolecules* 1997;30:574.